

NUMERICAL STUDY OF HEAT AND MASS TRANSFER OPTIMIZATION IN A 3-D INCLINED SOLAR DISTILLER

by

***Kaouther GHACHEM^a, Chamseddine MAATKI^a, Lioua KOLSI^{b,a*},
Naif ALSHAMMARI^b, Hakan F. OZTOP^c, Mohamed Naceur BORJINI^a,
Habib BEN AISSIA^a, and Khaled AL-SALEM^d***

^a Energy Engineering Department, National School of Engineering of Monastir,
University of Monastir, Monastir, Tunisia

^b Mechanical Engineering Department, College of Engineering, Hail University,
Hail City, Saudi Arabia

^c Department of Mechanical Engineering, Technology Faculty, Firat University, Elazig, Turkey

^d Department of Mechanical Engineering, College of Engineering, King Saud University,
Riyadh, Saudi Arabia

Original scientific paper

<https://doi.org/10.2298/TSCI150323161G>

A numerical study of the 3-D double-diffusive natural convection in an inclined solar distiller was established. The flow is considered laminar and caused by the interaction of thermal energy and the chemical species diffusions. The governing equations of the problem, are formulated using vector potential-vorticity formalism in its 3-D form, then solved by the finite volumes method. The Rayleigh number is fixed at $Ra = 10^5$ and effects of the buoyancy ratio and inclination are studied for opposed temperature and concentration gradients. The main purpose of the study is to find the optimum inclination angle of the distiller which promotes the maximum mass and heat transfer.

Key words: *solar distiller, 3-D study, double-diffusive convection, cavity inclination*

Introduction

In engineering, natural convection holds a great importance. In fact, solar collectors, furnaces, building heating and cooling system, heat exchangers are the typical applications of heat transfer and buoyancy-induced flow. Many researches, both experimentally and numerically, focus on the study of natural convection and/or mass transfer in inclined enclosures. The double-diffusive convection, which takes place when compositionally driven buoyant convection and thermally driven buoyant convection occur simultaneously, arises in a very wide range of fields such as oceanography, astrophysics, chemical vapor transport process, drying process, crystal growth process, etc. Many studies are published in this fields include the work of Ostrach [1], Costa [2, 3], and Nishimura *et al.* [4]. Different enclosure geometries were studied in these researches including square, parallelogram, and rectangular enclosures. Chouikh *et al.* [5] studied numerically the natural convection flow resulting from the combined buoyancy effects of thermal and mass diffusion in an inclined glazing cavity with differentially heated side walls.

* Corresponding author, e-mail: lioua_enim@yahoo.fr

The numerical approach endorsed the authors to analyze the complex natural convection flow situations arising in the inclined glazing cavity and to evaluate the effect of different parameters on the solar still performance. Nithyadevi and Yang [6] studied numerically the effect of double-diffusive natural convection of water in a partially heated enclosure with Soret and Dufour coefficients around the density maximum. The effect of the different parameters (thermal Rayleigh number, center of the heating location, density inversion parameter, buoyancy ratio number, Schmidt number, and Soret and Dufour coefficients) on the flow pattern and heat and mass transfer has been discussed.

However, few studies are interested in the 3-D double-diffusive natural convection. Sezai and Mohamed [7] studied thermosolutal natural convection in a cubic enclosure subject to horizontal and opposing gradients of heat and solute, they indicate that the double-diffusive flow in enclosures is strictly 3-D for a certain ranges of Rayleigh number, Lewis number, and buoyancy ratio. The same configuration was studied by Abidi *et al.* [8] but with heat and mass diffusive horizontal walls. They mentioned that the effect of the heat and mass diffusive walls is found to reduce the transverse velocity for the thermal buoyancy-dominated regime and to increase it considerably for the compositional buoyancy-dominated regime.

The performance of a solar distiller could be ameliorated by many parameters such as depth of water, glass cover angle, fabrication materials, temperature of water in the basin and insulation thickness, *etc.* In fact with the aim to maximize the distillate productivity of the apparatus over current solar stills, Naim [9] developed a single-stage solar desalination spirally-wound module of original design that makes use of both the latent heat of condensation of the formed vapor and the sensible heat of the concentrated solution, in preheating the incoming saline water. For the solar desalination of brackish water, the most used technology is the capillary film distiller which is composed of identical cells of evaporation-condensation Boucekima *et al.* [10, 11] and Boucekima [12]. Ben Snoussi *et al.* [13] studied this configuration by simulating numerically the natural convection in 2-D rectangular cavities. Results show that the flow, mass and thermal fields are strongly dependent on Rayleigh number and aspect ratio. A recent detailed review on active solar distillation procedures and modeling can be found in the work of Sampathkumar *et al.* [14]. Ghachem *et al.* [15] studied the numerically double-diffusive natural convection and entropy generation in 3-D solar distiller with an aspect ratio equal to two. They found that the variation of the buoyancy ratio affects significantly the isotherms distributions, iso-concentrations and the flow structure. Particularly for $N = 1$, the flow is completely 3-D. Besides, they found that all kinds of entropy generations present a minimum for $N = 1$. This result is due to the competition between thermal and compositional forces. These entropies rise considerably when N grows. On the one hand, the maximum of Bejan number is found for $N = 1$ which indicated the domination of heat and mass irreversibility's. Outside, friction irreversibility's are largely dominant. On the other hand, distribution of local Nusselt numbers changes with changing buoyancy ratio and take a complex structure for $N = 1$. The present work presents a numerical study of heat and mass transfer in an inclined solar distiller submitted to opposing temperature and concentration buoyancy forces. Recently, Alvarado-Juarez *et al.* [16, 17] studied numerically the heat and mass transfer in a solar still device especially the effect of the glass cover in such device. Authors focused their attention to the energy transmitted through the glass and they found that it is modified the flow pattern, and increases simultaneously the viscosity, the Nusselt and Sherwood numbers. The variation of the inclination angle increase the convection Nusselt and Sherwood numbers and the most suitable case for the solar still was an aspect ratio equal to five and an inclination angle between 6.67° and 20° . Chen *et al.* [18] studied numerically the entropy generation of turbulent double-diffu-

sive natural convection of nanofluid in a rectangular enclosure. They found that the total entropy generation of double-diffusive convection of nanofluid will reach its minimum when $N = 1$. It is different from its air counterpart. In double-diffusive convection of air, the total entropy is always a monotonic increasing function of N .

Mathematical formulation

Figure 1 presents the considered physical system which is composed of a square basic parallelepiped, with aspect ratio $F = H/W$ equal to 2. Different and uniform temperatures and concentrations are imposed on two vertical walls, where the thermal and compositional buoyancy forces are opposite (opposing flow) retards the force, *i. e.*, opposing flow. All the other walls are considered adiabatic. The hot wall warms up by the solar radiation inducing the evaporation of water film, the vapor thus produced mixes with the air then condenses when it reaches the cold wall. The fluid contained in the cavity is assumed incompressible and the flow follows the Boussinesq approximation.

The governing equations describing the double-diffusive natural convection are equations of continuity, of momentum, of energy and species diffusion:

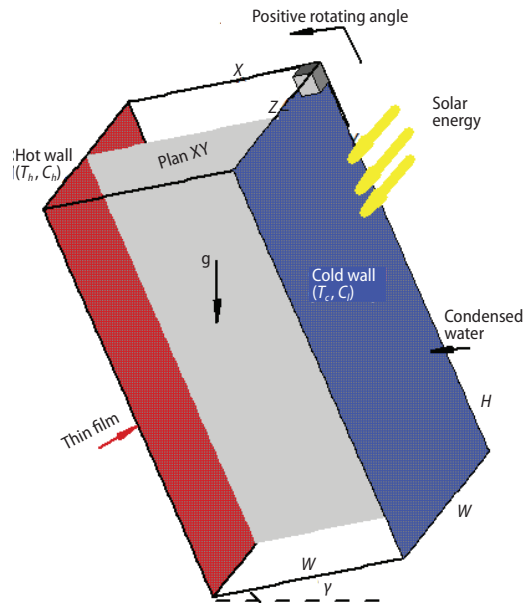


Figure 1. Physical model

$$\nabla \bar{V}' = 0 \tag{1}$$

$$\frac{\partial \bar{V}'}{\partial t'} + (\bar{V}' \cdot \nabla) \bar{V}' = -\frac{1}{\rho} \nabla P' + \nu \Delta \bar{V}' + \beta_t (T' - T_o) \bar{g} + \beta_c (C' - C_o) \bar{g} \tag{2}$$

$$\frac{\partial T'}{\partial t'} + \bar{V}' \cdot \nabla T' = \alpha \nabla^2 T' \tag{3}$$

$$\frac{\partial C'}{\partial t'} + \bar{V}' \cdot \nabla C' = D \nabla^2 C' \tag{4}$$

In order to eliminate the pressure term, which is delicate to treat, the numerical method used in this work is based on the vorticity – vector potential formalism ($\bar{\omega}' - \bar{\omega}$). For this, one applies the rotational to the equation of momentum. The vector potential and the vorticity are, respectively, defined by the two following relations:

$$\bar{\omega}' = \nabla \times \bar{V}' \quad \text{and} \quad \bar{V}' = \nabla \times \bar{\psi}' \tag{5}$$

Based on the dimensionless variables the governing equations can be written:

$$-\bar{\omega} = \nabla^2 \bar{\psi} \tag{6}$$

$$\frac{\partial \bar{\omega}}{\partial t} + (\bar{\nabla} \nabla) \bar{\omega} - (\bar{\omega} \nabla) \bar{\nabla} =$$

$$= \Delta \bar{\omega} + \text{Ra Pr} \left\{ \begin{array}{l} \left(\frac{\partial T}{\partial z} + N \frac{\partial C}{\partial z} \right) \cos \gamma \\ \left(-\frac{\partial T}{\partial z} - N \frac{\partial C}{\partial z} \right) \sin \gamma \\ \left[\left(-\frac{\partial T}{\partial x} \cos \gamma + \frac{\partial T}{\partial y} \sin \gamma \right) + N \left(-\cos \gamma \frac{\partial C}{\partial x} + \sin \gamma \frac{\partial C}{\partial y} \right) \right] \end{array} \right\} \quad (7)$$

$$\frac{\partial T}{\partial t} + \bar{\nabla} \nabla T = \nabla^2 T \quad (8)$$

$$\frac{\partial C}{\partial t} + \bar{\nabla} \nabla C = \frac{1}{\text{Le}} \nabla^2 C \quad (9)$$

where

$$\text{Pr} = \frac{\nu}{\alpha} \quad \text{Ra} = \frac{g \beta_l W^3 (T_h' - T_c')}{\alpha \nu} \quad N = \frac{\beta_c (C_h' - C_l')}{\beta_l (T_h' - T_c')} \quad \text{Le} = \frac{\alpha}{D} = \frac{\text{Sc}}{\text{Pr}}$$

For $N = 0$, there is no mass diffusion and thermal and species diffusions are assumed to be opposed. For $0 < N < 1$ the flow is thermal dominated and for $N > 1$ the flow is compositional dominated.

The initial and boundary conditions are written as follows.

- Temperature: $T = 1$ at $x = 0$, $T = 0$ at $x = 1$, $\partial T / \partial n = 0$ on other walls (adiabatic).
- Concentration: $C = 1$ at $x = 0$, $C = 0$ at $x = 1$, $\partial C / \partial n = 0$ on other walls (impermeable).
- Vorticity: $\omega_x = 0$, $\omega_y = -\partial V_z / \partial x$, $\omega_z = \partial V_y / \partial x$ at $x = 0$ and 1 , $\omega_x = \partial V_z / \partial y$, $\omega_y = 0$, $\omega_z = -\partial V_x / \partial y$ at $y = 0$ and 1 , $\omega_x = -\partial V_y / \partial z$, $\omega_y = \partial V_x / \partial z$, $\omega_z = 0$ at $z = 0$ and 1 .
- Vector potential: $\partial \psi_x / \partial x = \psi_y = \psi_z = 0$ at $x = 0$ and 1 , $\psi_x = \partial \psi_y / \partial y = \psi_z = 0$ at $y = 0$ and 1 , $\psi_x = \psi_y = \partial \psi_z / \partial z = 0$ at $z = 0$ and 1 .
- Velocity: $V_x = V_y = V_z = 0$ on all walls.

The local Nusselt and Sherwood numbers are given by:

$$\text{Nu} = \frac{\partial T}{\partial x} \Big|_{x=0,1} \quad \text{and} \quad \text{Sh} = \frac{\partial C}{\partial x} \Big|_{x=0,1} \quad (10)$$

The average Nusselt and Sherwood numbers, on the active walls are expressed by:

$$\bar{\text{Nu}} = \int_0^1 \int_0^1 \text{Nu} \, \partial y \, \partial z \quad \text{and} \quad \bar{\text{Sh}} = \int_0^1 \int_0^1 \text{Sh} \, \partial y \, \partial z \quad (11)$$

Validation test

The validation of the present numerical solution is done by a comparison with the 2-D results of Nishimura *et al.* [4]. In fact figs. 2 and 3 show the isotherms, iso-concentration, and velocity vector projection in the XY-plan for $N = 0.8$ and $N = 1.3$. These results are in good agreement with those of Nishimura *et al.* [4]. It is noted that in 3-D configurations the projections of velocity vector are not closed compared with 2-D configurations.

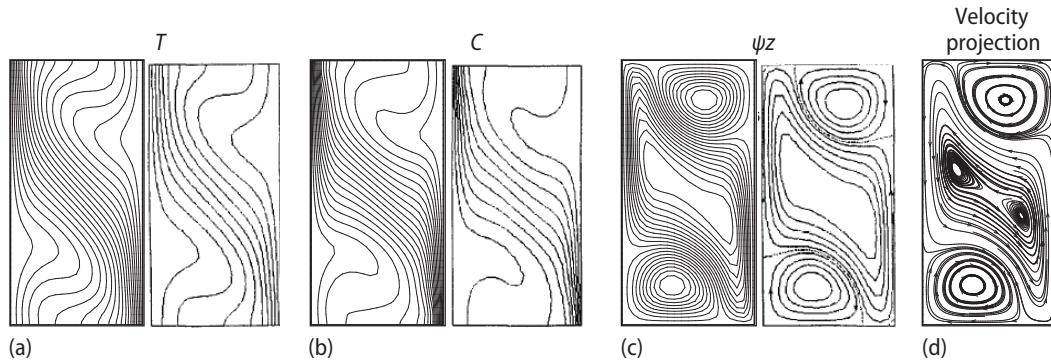


Figure 2. Comparison between results of the present work (left) and those of Nishimura *et al.* [4] (right) for $N = 0.8$; (a) isotherms, (b) iso-concentration, (c) z-component of vector potential, (d) velocity projection in the XY-plan

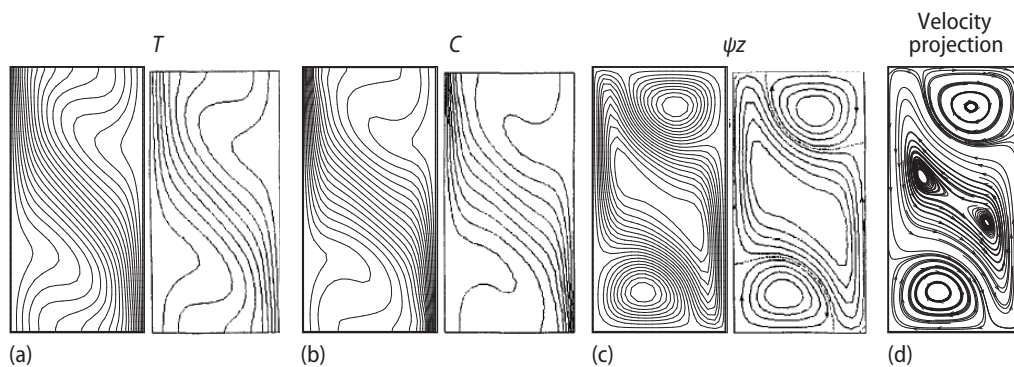


Figure 3. Comparison between results of the present work (left) and those of Nishimura *et al.* [4] (right) for $N = 1.3$; (a) isotherms, (b) iso-concentration, (c) z-component of vector potential, and (d) velocity projection in the XY-plan

Results and discussion

Numerical results are presented for $Pr = 0.71$ and $Le = 0.85$ which cover water vapor diffusion into air. The Rayleigh number is fixed at $Ra = 10^5$, and the buoyancy ratio is varied from $N = 0.8$ to 1.5 by the respect of the condition of opposing flow. Two parts are presented. The first one will discuss the effect of the buoyancy ratio on the flow structure and the heat and mass transfer for a vertical distiller ($\gamma = 0^\circ$) although the second part will present the effect of the variation of the inclination angle of the solar distiller on the flow structure and the heat and mass transfer for three buoyancy ratios $N = 0.8$, $N = 0.95$, and $N = 1.5$.

Effect of the buoyancy ratio on the flow structure and heat and mass transfer for $\gamma = 0^\circ$

The main purpose of this part is to highlight the behavior of the flow structure and the heat and mass transfer by the variation of N . For this, the distiller is maintained vertical at $\gamma = 0^\circ$.

Figure 4 shows the projection of the velocity vector in the central plan for different buoyancy ratio at $\gamma = 0^\circ$. For $N = 0.8$, fig. 4(a), the flow is thermal dominated characterized with one central vortex which turns in the clockwise. When $N = 0.95$, fig. 4(b), three vortex are noted. The first is a thermal vortex witch situated in the core of the cavity and turning in the clockwise.

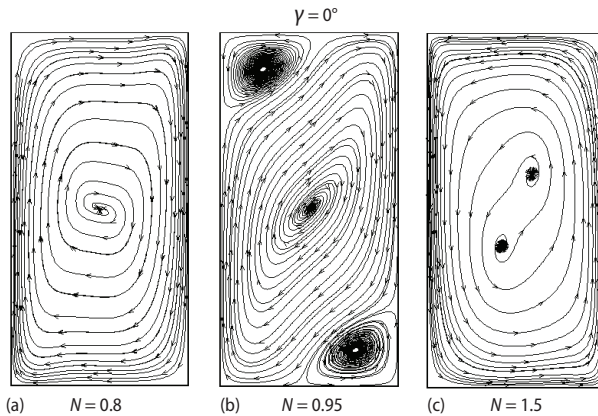


Figure 4. Velocity vector projection in the XY-plan for $\gamma = 0^\circ$ and different N

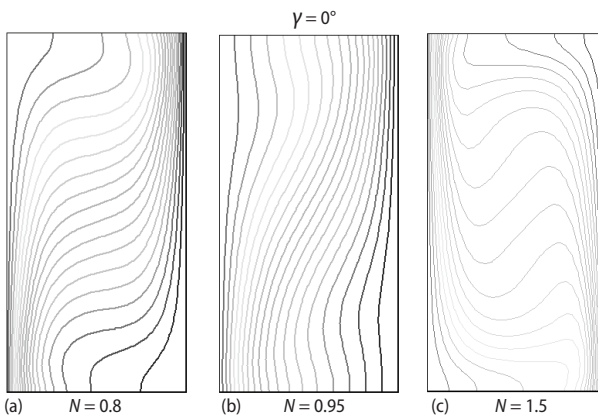


Figure 5. Plots of isotherms in the XY-plan for $\gamma = 0^\circ$ and different N

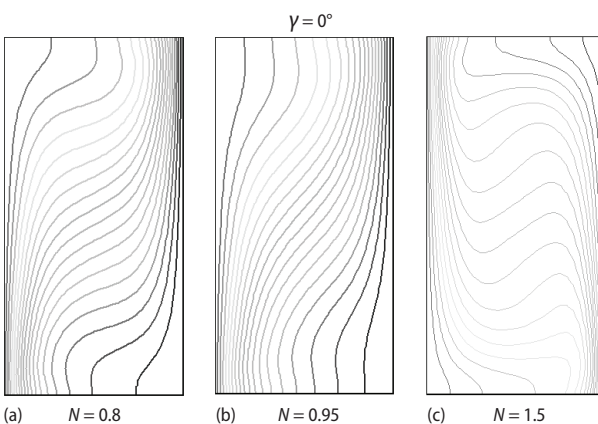


Figure 6. Plots of iso-concentration in the middle XY-plan for $\gamma = 0^\circ$ and different N

The secondary two solutal vortex are situated in the top corner of the hot wall and the lower corner of the cold wall. They turn counter clockwise. For $N = 1.5$, fig. 4(c), the flow is solutal dominated and it is characterized by one center vortex turning counter clockwise with two cells turning in the same direction.

Figures 5 and 6 show the isotherms and iso-concentration in the middle XY-plan for $\gamma = 0^\circ$. When $N = 0.8$, figs. 5(a) and 6(a), the isotherms and the iso-concentration are vertical near the active walls and distorted in the core of the cavity. When $N = 0.95$, figs. 5(b) and 6(b), the thermal and the solutal gradients decrease inducing a decrease of the heat and mass transfer. For $N = 1.5$, figs. 5(c) and 6(c), the flow is compositional dominated. The thermal and solutal gradients are important especially near the top part of the hot wall. Although in the core region of the cavity, they present a vertical stratification.

Figure 7 shows the variation of the average Nusselt and Sherwood numbers as function of N , for $\gamma = 0^\circ$. The minimum of the heat and mass transfer are detected for $N = 1$. This result is earlier found by Sezai and Mohamed [7] for $Pr = 10$ and $Le = 10$. When $N > 1$, case of compositional dominated flow, the mean Nusselt and Sherwood numbers increase with the increasing of N in the negative direction.

Effect of inclination angle on the flow structures for $N = 0.95$ and $N = 1.5$

Figures 8-10 shows the projection of the velocity vector in the central plan for different γ . The buoyancy ratio is fixed firstly at 0.8 then at 0.95 and finally at 1.5.

For $N = 0.8$, $N = 0.95$, and $N = 1.5$, an inclination of the so-

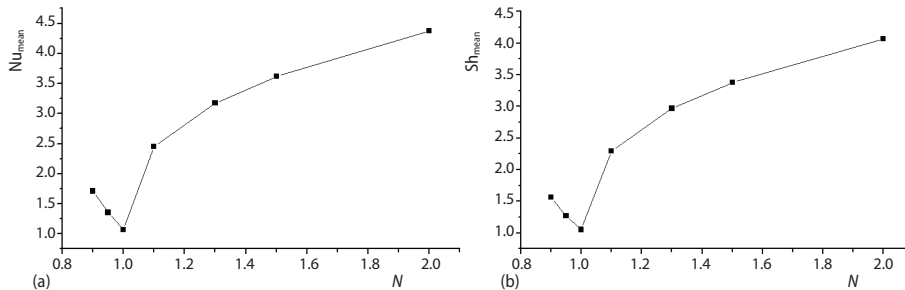


Figure 7. Effect of buoyancy ratio on Nu_{mean} and Sh_{mean} for $\gamma = 0^\circ$

lar distiller by $\gamma = 10^\circ$, has no effect on the streamlines distribution. They are similar to those of $\gamma = 0^\circ$, fig. 4.

For $N = 0.8$ and by the increase of the inclination angle, the regime evolved from one thermal vortex, figs. 8(a) and 8(b), to two vortices turning in the same direction, fig. 8(c).

For $N = 0.95$ and $\gamma = 30^\circ$, fig. 9(b), the two solutal vortex that appear for $\gamma = 10^\circ$, fig. 9(a), become smaller and closer to the top corner of the hot wall for one, and to the bottom corner of the cold wall for the other. For $\gamma = 70^\circ$, fig. 9(c), the solutal vortex disappear totally and one central thermal vortex takes place and turning in the clockwise. In conclusion, the deviation of the distiller, when $N = 0.95$, promotes the convection mode despite the solutal contribution.

In the case of $N = 1.5$, increasing the inclination angle reduces the solutal vortices from two to one, fig. 10(a). Furthermore, it is noted the development of a small thermal vortex located near the top corner of the cold wall where $\gamma = 30^\circ$ and slightly shifted to the top of the adiabatic wall when $\gamma = 70^\circ$, this effect is due to the inclination.

Isotherms and iso-concentration in XY-plan, for $N = 0.8, 0.95$, and 1.5 are, respectively, presented on figs. 11-16. First off all, it is noted that the maps of isothermal and iso concentration are similar for all the studied cases. This is justified by the value of Lewis number which is near of the unity.

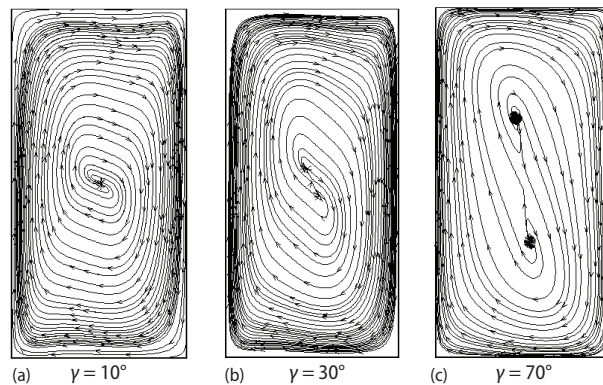


Figure 8. Projection of the velocity vector in the XY-plan for $N = 0.8$

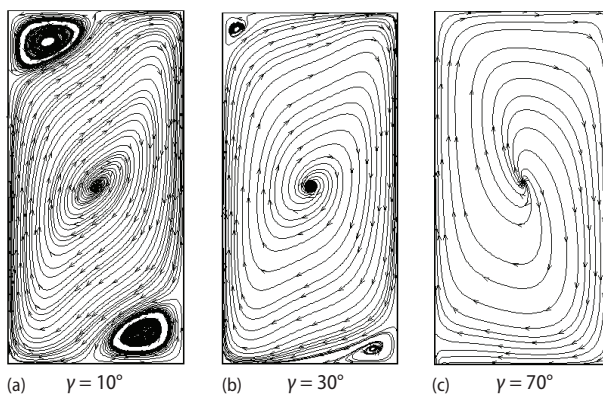


Figure 9. Projection of the velocity vector in the XY-plan for $N = 0.95$

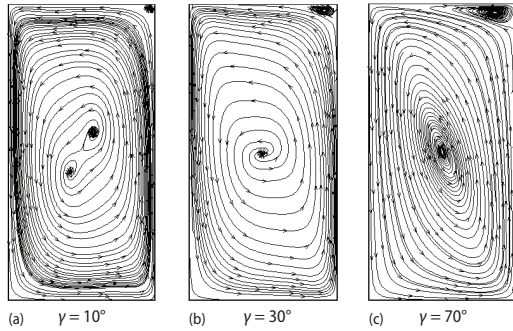


Figure 10. Projection of the velocity vector in the XY-plan for $N = 1.5$

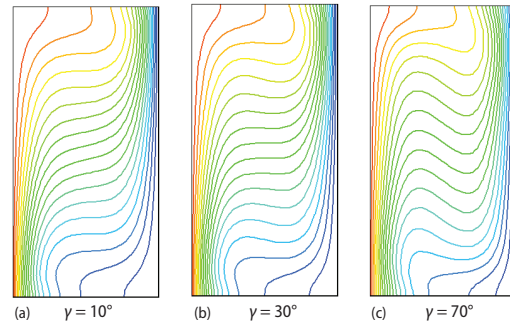


Figure 11. Isotherms in the XY-plan for $N = 0.8$

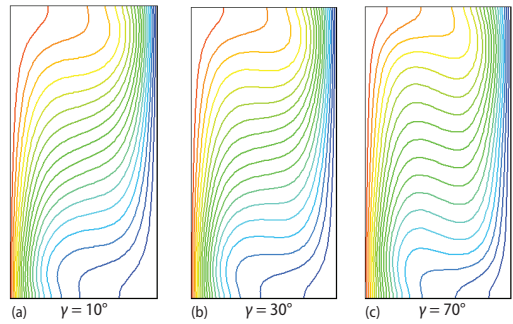


Figure 12. Iso-concentration in the XY-plan for $N = 0.8$

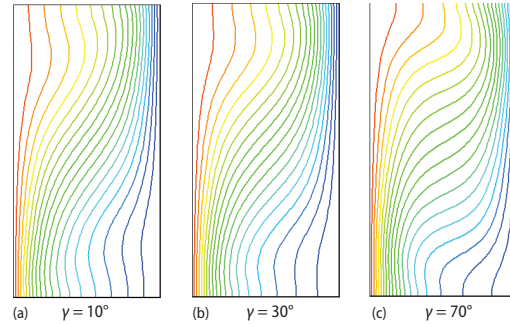


Figure 13. Isotherms in the XY-plan for $N = 0.95$

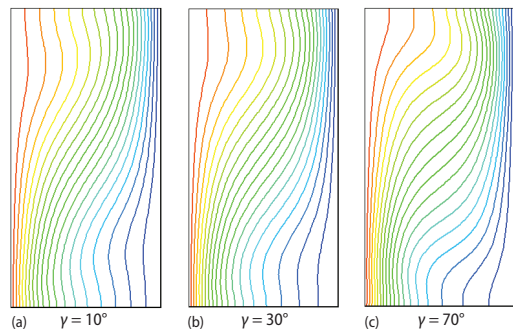


Figure 14. Iso-concentration in the XY-plan for $N = 0.95$

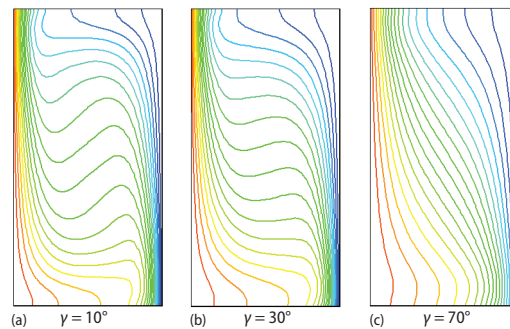


Figure 15. Plots of isotherms in the XY-plan for $N = 1.5$

For $N = 0.8$, the regime is thermal dominated. When $\gamma = 10^\circ$, the isotherms and the iso-concentration are vertical near the active walls and they are inclined in the core of the cavity. By the increase of $\gamma = 30^\circ$, a vertical stratification of the isotherms (iso-concentrations) takes place in the central region of the cavity. For $\gamma = 70^\circ$, isotherms (iso-concentrations) become more distorted in the core region.

Firstly, it is noted that the thermal and solutal gradient slightly increase near the active walls and decrease in the core region by the increase of the inclination angle. For $\gamma = 70^\circ$, figs. 13(c) and 14(c), the isotherms and iso-concentration are distorted in the core region.

In contrast with the previous cases, when $N = 1.5$, Figs. 15 and 16, the high thermal and solutal gradients become situated near the top of the hot wall and the bottom of the cold wall. The isotherms and iso-concentration are verticals near the active walls and they are distorted in the core region, $\gamma = 10^\circ$.

For $\gamma = 30^\circ$, a small decrease of the solutal and thermal gradients are noticed near the active walls. Also, a vertical stratification appears for the isotherms and iso-concentration. When $\gamma = 70^\circ$, the thermal and solutal gradient decreases near the active walls and the isotherms and iso-concentration become inclined and parallel.

Figure 17 shows the evolution of the maximum of z-component velocity, $V_{z_{max}}$, for $N = 0.8$, $N = 0.95$, and $N = 1.5$ for the different positive angles. Firstly, the 3-D character increases for $N = 0.8$ from $\gamma = 0^\circ$ to $\gamma = 60^\circ$. After that, it slightly decreases for $\gamma = 70^\circ$ and finally it increases for $\gamma = 80^\circ$ and $\gamma = 90^\circ$.

For $N = 0.95$, the evolution of $V_{z_{max}}$ has an optimum at $\gamma = 70^\circ$ after which it decreases. For $N = 1.5$, the inclination angle causes a significant decrease of $V_{z_{max}}$ from 11.82 (for $\gamma = 0^\circ$) to 0.31 (for $\gamma = 90^\circ$). This means a reduction in the 3-D nature of the flow.

Figures 18 and 19 present simultaneously the variation of the mean Nusselt and Sherwood numbers for different inclination angles. Firstly, one notes that the variations of these numbers have quietly the same behavior with a major of the Nusselt number values. Besides, when γ is negative and $N = 0.95$, values of Nu and Sh decrease. However, when γ is positive

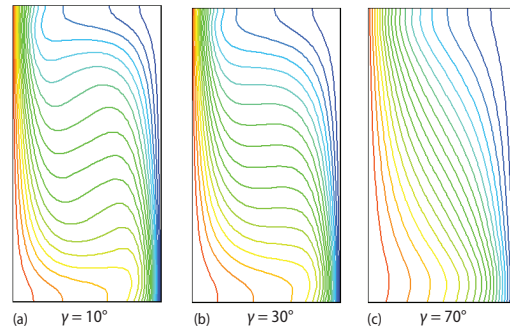


Figure 16. Plots of iso-concentration in the XY-plan for $N = 1.5$

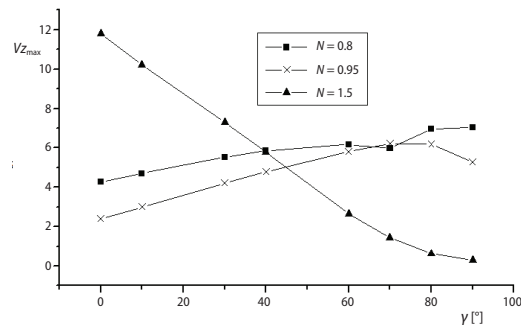


Figure 17. Evolution of Z velocity by the inclination angle for different buoyancy ratio

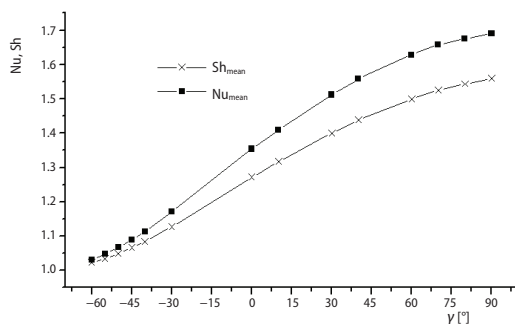


Figure 18. Variation of the mean Nusselt and Sherwood numbers for $N = 0.95$ and different angles

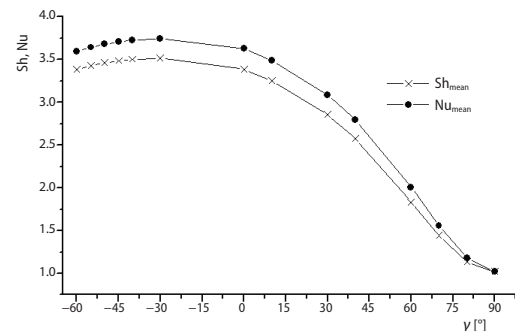


Figure 19. Variation of the mean Nusselt and Sherwood numbers for $N = 1.5$ and different angles

their values increase by the increase of γ . In the other hand, when the flow is compositional dominated ($N = 1.5$) a slight increase of \overline{Nu} and \overline{Sh} are located at $\gamma = -30^\circ$. Nevertheless, when γ is positive a great decrease is detected.

A good correlation can be found for the two variations.

- For $N = 0.95$: the correlation of the mean Nusselt is given by:

$$\overline{Nu} = 1.3604 + 0.00512\gamma - 1.405 \cdot 10^{-5} \gamma^2$$

and the correlation of the mean Sherwood number is given by:

$$\overline{Sh} = 1.2768 + 0.00408\gamma - 8.8036 \cdot 10^{-6} \gamma^2$$

- For $N = 1.5$: the correlation of the mean Nusselt is given by:

$$\overline{Nu} = 3.3245 - 0.012\gamma - 1.89 \cdot 10^{-4} \gamma^2$$

and the correlation of the mean Sherwood number is given by:

$$\overline{Sh} = 3.5827 - 0.0124\gamma - 2.0485 \cdot 10^{-4} \gamma^2$$

The correlation coefficient for these equations is greater than 99%.

Conclusions

The 3-D thermo solutal natural convection in an inclined solar distiller subject to horizontal and opposing gradients of heat and solute is modeled and solved numerically using finite volume method. Buoyancy ratio and inclination angle are varied through the study in order to gain new insights into the variation of mass and heat transfer from one side and into the flow structure in the other side.

The main finding of the current investigation can be summarized as follows.

- Upon increasing the magnitude of N in the negative direction, a secondary flow is set up in the transverse plan ($N = 0.95$).
- When the magnitude of N increases, a reversal of the main flow rotation occurs, resulting of the increasing dominance of solutal over the thermal buoyancy ($N = 1$). This can be the consequence of the minimum seen in the variation of the mean Nusselt and Sherwood numbers. It is noted that the solutal dominance takes place for $N = 1.4$ in the 2-D model (Sezai and Mohamed [7]).
 - For $N = 0.8$ and by the increase of the inclination angle
The regime evolved from one thermal vortex with one cell to another with two vortexes turning all in the clockwise direction. The isotherms and iso-concentration are more distorted
 - For $N = 0.95$
Upon increasing the magnitude of γ the secondary flow disappears gradually the deviation of the distiller, promotes the convection mode despite the solutal contribution. The \overline{Nu} and \overline{Sh} numbers increase by the increase of γ in the positive sense and decrease in the opposite one.
 - For $N = 1.5$
The maximum of \overline{Nu} and \overline{Sh} numbers is find at $\gamma = -30^\circ$

Acknowledgment

Fifth and last authors extend their appreciation to the International Scientific Partnership Program ISPP at King Saud University for funding this research work through ISPP#0030.

Nomenclature

C	–dimensionless concentration, [$= (C' - C_l') / (C_h' - C_l')$], [-]	W	–enclosure width, [m]
D	–mass diffusivity, [m^2s^{-1}]	x, y, z	– Cartesian co-ordinates
g	–acceleration of gravity, [ms^{-2}]	<i>Greek symbols</i>	
H	–enclosure height, [m]	α	–thermal diffusivity, [m^2s^{-1}]
Le	–Lewis Number, [-]	β	–expansion coefficient, [m^3kg^{-1}]
N	–buoyancy ratio	γ	–inclination angle, [$^\circ$]
Pr	–Prandtl number, [-]	ρ	–density, [kgm^{-3}]
Ra	–Rayleigh number, [-]	ν	–kinematic viscosity, [m^2s^{-1}]
Sc	–Schmidt number, [-]	$\vec{\psi}$	–dimensionless vector potential ($= \vec{\psi}' / \alpha$), [-]
Sh	–Sherwood number, [-]	$\vec{\omega}$	–dimensionless vorticity ($= \vec{\omega}' \alpha / l^2$), [-]
T	–dimensionless temperature, [$= (T' - T'_c) / (T'_h - T'_c)$], [-]	<i>Subscripts</i>	
T'_c	–cold temperature, [K]	c	–compositional
T'_h	–hot temperature, [K]	t	–thermal
t	–dimensionless time ($= t' \alpha / l^2$), [-]	o	–initial
\vec{V}	–dimensionless velocity vector ($= \vec{V}' l / \alpha$), [-]	<i>Superscript</i>	
		'	–dimensional variable

References

- [1] Ostrach, S., Natural Convection with Combined Driving Forces, *Phys. Chem. Hydrodyn.*, 1 (1980), 4, pp. 233-247
- [2] Costa, V. A. F., Double Diffusive Natural Convection in a Square Enclosure with Heat and Mass Diffusive Walls, *Int. J. Heat Mass Transfer*, 40 (1997), 17, pp. 4061-4071
- [3] Costa, V. A. F., Double-Diffusive Natural Convection in Parallelogrammic Enclosures, *Int. J. Heat Mass Transfer*, 47 (2004), 14-16, pp. 2913-2926
- [4] Nishimura, T., et al., Oscillatory Double Diffusive Convection in a Rectangular Enclosure with Combined Horizontal Temperature and Concentration Gradients, *Int. J. Heat Mass Transfer*, 41 (1998), 11, pp. 1601-1611
- [5] Chouikh, R., et al., Numerical Study of the Heat and Mass Transfer in Inclined Glazing Cavity: Application to a Solar Distillation Cell, *Renew. Energ.*, 32 (2007), 9, pp. 1511-1524
- [6] Nithyadevi, N., Yang, R.-J., Double Diffusive Natural Convection in a Partially Heated Enclosure with Soret and Dufour Effects, *Int. J. Heat Fluid Flow*, 30 (2009), 5, pp. 902-910
- [7] Sezai, I., Mohamed, A. A., Double Diffusive Convection in a Cubic Enclosure with Opposing Temperature and Concentration Gradients, *Physics of Fluids*, 12 (2000), 9, pp. 2210-2223
- [8] Abidi, A., et al., Effect of Heat and Mass Transfer through Diffusive Walls on Three-Dimensional Double-Diffusive Natural Convection, *Numerical Heat Transfer, Part A: Applications*, 53 (2008), 12, pp. 1357-1376
- [9] Naim, M. M., Solar Desalination Spirally-Wound Module, in: *Alternative Energy Sources VIII* (Ed. T. N. Veziroglu), Hemisphere Publishing, N. Y., USA, 1987, pp. 571-580
- [10] Boucekima, B., et al., Theoretical Study and Practical Application of the Capillary Film Solar Distiller, *Renewable Energy*, 16 (1999), 1-4, pp. 795-799
- [11] Boucekima, B., et al., Theoretical Study and Practical Application of the Capillary Film Solar Distiller (in French), *Int. J. Therm. Sci.*, 39 (2000), 3, pp. 442-459
- [12] Boucekima, B., A Small Solar Desalination Plant for the Production of Drinking Water in Remote Arid Areas of Southern Algeria, *Desalination*, 159 (2003), 2, pp. 197-204
- [13] Ben Snoussi, L., et al., Numerical Study of the Natural Convection Flow Resulting from the Combined Buoyancy Effects of Thermal and Mass Diffusion in a Cavity with Differentially Heated Side Walls, *Desalination*, 182 (2005), 1-3, pp. 143-150
- [14] Sampathkumar, K., et al., Active Solar Distillation – A Detailed Review, *Renewable and Sustainable Energy Reviews*, 14 (2010), 6, pp. 1503-1526
- [15] Ghachem, K., et al., Three-Dimensional Double Diffusive Free Convection and Irreversibilities Studies in a Solar Distiller, *International Communications in Heat and Mass Transfer*, 39 (2012), 6, pp. 869-876

- [16] Alvarado-Juarez, R., *et al.*, Numerical Study of Heat and Mass Transfer in a Solar Still Device: Effect of the Glass Cover, *Desalination*, 359 (2015), Mar., pp. 200-211
- [17] Alvarado-Juarez, R., *et al.*, Numerical Study of Conjugate Heat and Mass Transfer in a Solar Still Device, *Desalination*, 325 (2013), Sept., pp. 84-94
- [18] Chen, S., *et al.*, Analysis of Entropy Generation in Double-Diffusive Natural Convection of Nanofluid, *International Journal of Heat and Mass Transfer*, 87 (2015), Aug., pp. 447-463